LA-UR- 99-215

Approved for public release; distribution is unlimited.

Title: ATOMISTIC STUDIES OF JOGGED SCREW DISLOCATIONS IN γ-TIAL ALLOYS

CONF-981104--

Author(s): K. Y. Chen
M. Li
S. J. Zhou

Submitted to: Materials Research Society, Fall Meeting, Boston, MA, Nov. 30-Dec. 4, 1998

Los Alamos
NATIONAL LABORATORY

DISCLAIMER

ATOMISTIC STUDIES OF JOGGED SCREW DISLOCATIONS IN γ-TIAL ALLOYS

K. Y. Chen*, M. Li*, S. J. Zhou**

*Theoretical Division and Center for Nonlinear Studies, Los Alamos National Laboratory, Los Alamos, NM 87545, USA
**Applied Theoretical and Computational Physics Division, Los Alamos National Laboratory, Los Alamos, NM 87545, USA

ABSTRACT

The behavior of jogged screw dislocations in γ-TiAl alloys has been investigated with large-scale molecular dynamics (MD) simulations. We find a new mechanism for formation of pinning points in jogged screw dislocations. We also find that the critical height for the jogs in the $\pm[\bar{1}10]$ directions on the (001) plane to move nonconservatively is between $3r_0$ and $4r_0$, where r_0 is the nearest neighbor distance of aluminum atoms. Interstitials and vacancies are created during the nonconservative motions of the jogs. In addition, the formation of dislocation dipole and loops around the jogs is also observed.

INTRODUCTION

Experimental results indicate that the anomalous yield stress of γ-TiAl alloys at ambient temperatures is closely associated with simple unit screw dislocations [1-4]. Recent work by Sriram *et al.* [1] showed that the deformation substructures at ambient temperatures are dominated by unit screw dislocations pinned by a number of jogs along screw character segments. Due to the compact core structures of screw dislocations in γ-TiAl alloys, the cross-slip and the double cross-slip, which play a major role in generating jogs, are profuse. Viguier *et al.* [2] suggested that a simple screw dislocation gliding on the primary as well as cross-slip planes is the intrinsic source for the formation of pinning points, and the pinning points can be erased by the lateral motion of superkinks. As one of the potential pinnings, a jog has a significant role in dislocation mobility. Investigating dynamic behaviors of jogs with different heights will be very important to understand the anomalous yield stress in γ-TiAl alloys. There have been some theoretical studies of nonconservative motion of jogs [5], but the detailed mechanism is poorly understood. With the current powerful computers, this problem can now be coped with [6,7]. In this paper, we are motivated to investigate jogged screw dislocations in γ-TiAl alloys by performing large-scale MD simulations.

SIMULATION PROCEDURE

The methodology of our large-scale MD simulations is briefly summarized here. We chose the embedded atom method (EAM) potentials for γ-TiAl alloys developed by Farkas [8]. These potentials were obtained by empirically fitting equilibrium lattice parameters, c/a ratio, heat of formation, elastic constants, etc.. Throughout the paper, we use as units the atomic mass m of aluminum, the distance r_0 between nearest neighbors of aluminum atoms (or titanium atoms), the energy unit ε. So the unit of time t_0 is determined by $t_0 = r_0\sqrt{m/\varepsilon}$. The time step is chosen to be $0.01t_0$. For the EAM potential used, the energy unit is ε=0.73 eV, t_0=1.7×10^{-13}s, a=3.95 Å, c=4.14 Å, and r_0=2.7 Å. In our simulations, each MD system is first allowed to relax for $10t_0$

without any loading. Then a constant shear strain rate, $\dot{\varepsilon}_{yz} = 5.4\times10^9 s^{-1}$, is exerted on the system for another $100t_0$. At t=$110t_0$, the shear stress σ_{yz} is 5.7×10^3 MPa. We have performed similar simulations with lower strain rate, and have found the basic physical processes unchanged. In this paper, we study the behavior of the jogged screw dislocations without the complications of thermal fluctuations, thus the initial temperature is set to be nearly zero (30 K). The constant-temperature MD integration scheme is implemented to maintain the system temperature at 30 K.

The γ-TiAl alloy presents an $L1_0$ configuration. The system size throughout this paper is chosen to be $L_x \times L_y \times L_z = 609\times211\times338\AA^3$, containing about 1.1 million atoms. Initially, we set the screw dislocation lines parallel to the [110] (z-axis) with a pair of jog segments in the $\pm[\bar{1}10]$ directions (see FIG01(a)). These two jogs attract each other. The Burgers vector is chosen as $\boldsymbol{b}=-b\hat{z}$ and the sense vector ξ of the screw dislocation is along the direction [110] (z-axis), so the screw dislocation lines can move along the $[1\bar{1}\bar{2}]$ direction (negative x-axis) on the $(1\bar{1}1)$ primary slip plane under the external shear strain rate $\dot{\varepsilon}_{yz}$ (see FIG01(b)). That the jog segments in the $\pm[\bar{1}10]$ directions on the (001) plane climb in the $[1\bar{1}\bar{2}]$ direction (negative x-axis) is defined as the forward nonconservative motion. Periodic boundary conditions are maintained in the [110] direction. The external shear strain rate $\dot{\varepsilon}_{yz}$ is exerted on $\pm y$ surfaces and the two $\pm x$ surfaces are set free. We chose the jogs lying on the (001) plane mainly for the computational simplicity. The conservative motion of a jog segment is much faster on the $(1\bar{1}1)$ slip plane than that on the (001) plane. That would cause the jog pair to annihilate in our MD computational cell in such a short time that the forward nonconservative jog motions do not have sufficient time to proceed. We found that the <110> jog on the (001) plane has dynamic behavior similar to that found on the $(1\bar{1}1)$ slip plane in larger MD systems (to be reported in future).

RESULTS AND DISCUSSIONS

We have investigated jogged screw dislocations of several different heights. Here the jogged screw dislocations of heights $4r_0$ and $15r_0$ will be discussed in detail to show

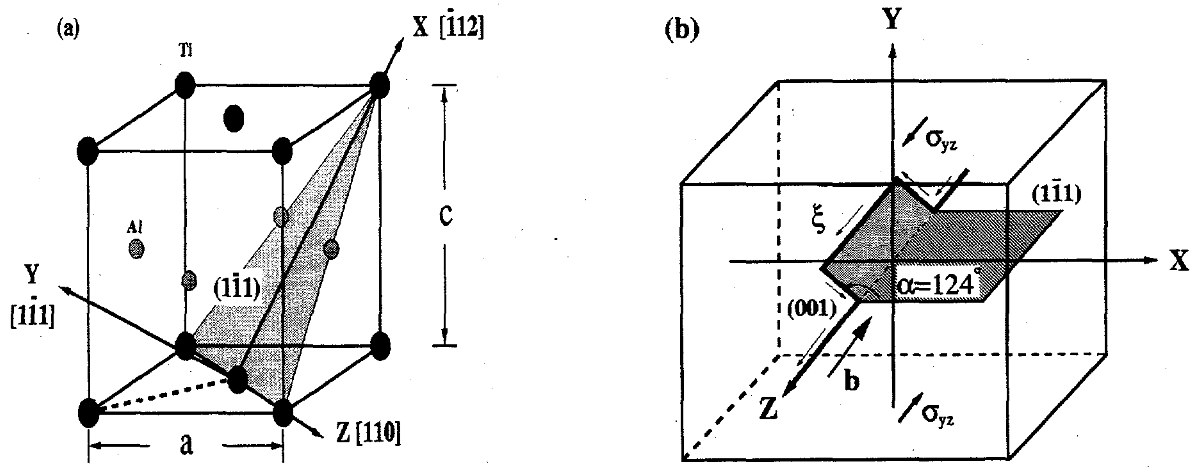

FIG01 (a) Schematic of the γ-TiAl crystal structure and the coordinate system. (b) Schematic of a jogged screw dislocation in the MD computational cell. The screw dislocation line lies parallel to the z-axis and its slip plane is the $(1\bar{1}1)$ plane (xz plane). The plane (001) where a pair of jogs are located, has an angle $\alpha=124^{\circ}$ with respect to the $(1\bar{1}1)$ slip plane.

the typical observations. We have found that under the shear strain rate $\dot{\varepsilon}_{yz} = 5.4\times10^{9}s^{-1}$, the critical height for the jog to move forward in a nonconservative way is between $3r_0$ and $4r_0$. So it is reasonable to choose the critical height as $3.5r_0$. FIG02 shows the evolution process of a jogged screw dislocation with the height $4r_0$. In the first $10t_0$, the two jogs as well as the screw dislocation segments relax on the (001) plane without any loading (FIG02(a)). As shown in FIG02(b), both of the jogs decompose gradually into small jogs with the jog heights ($\sim 2r_0$) less than the critical length ($\sim 3.5r_0$). In addition, due to the attractive interaction between a pair of jogs with the opposite sign, these small, newly generated jogs move toward each other. Under the external shear stress σ_{yz} (after $10t_0$), the newly generated jogs move nonconservatively on the primary slip plane $(1\bar{1}1)$. Similar to our previous observations for the jog with the height $2r_0$ [9], interstitials and vacancies are created during the forward nonconservative motion in the $[1\bar{1}\bar{2}]$ direction. A jog that can generate vacancies is defined as a vacancy jog. Similarly, a jog that can create interstitials is defined as an interstitial jog. In addition to the forward nonconservative motion, we find that the jog also moves conservatively along the $[\bar{1}\bar{1}0]$ direction on the (001) plane. It can be clearly seen in FIG02(c) that the vacancy tube V_1 formed during the jog nonconservative motion is aligned in the $[0\bar{1}\bar{1}]$ direction. FIG02(c) also shows that the screw dislocation segments bow out around the jogs on the primary slip plane $(1\bar{1}1)$. Based on the Peach-Koehler formula $\boldsymbol{F}=(\boldsymbol{b}\bullet\sigma)\times\xi$ [5], we can identify that the external force $\boldsymbol{F}$ exerted on the jog segments due to σ_{yz} is along z-axis ([110]) for the vacancy jogs and is along negative z-axis ($[\bar{1}\bar{1}0]$) for the interstitial jogs. Thus the Peach- Koehler forces would make the vacancy jogs deviate from the $[0\bar{1}\bar{1}]$ direction and the interstitial jogs deviate from the $[1\bar{1}\bar{2}]$ direction. However, FIG02(c) shows that under the shear strain rate $\dot{\varepsilon}_{yz} = 5.4\times10^{9}s^{-1}$ the Peach-Koehler forces have no strong effect on the conservative motions of interstitial jog J_{I1} and vacancy jog J_{V1}. It is known that the formation energy of an interstitial is higher than that of a vacancy [10]. The current applied shear strain rate $\dot{\varepsilon}_{yz}$ is not large enough to move the interstitial jog J_{I1} along the $[\bar{1}\bar{1}0]$ direction. FIG02(c) also shows that the newly generated interstitial jog J_{I2} and vacancy jog J_{V2} are closer to each other. So their attractive interaction is stronger. Due to the attractive interaction of these jogs, the lateral conservative motion of interstitial jog J_{I2} along the $[\bar{1}\bar{1}0]$ direction occurs on the (001) plane. This causes the interstitial jog J_{I2} to move along approximately along the $[0\bar{1}\bar{1}]$ direction. Similarly, the vacancy jog J_{V2} bends to some extent towards the interstitial jog J_{I2}. At $t=50t_0$, the interstitial cluster I_2 and the vacancy tube V_2 disappear gradually (FIG02(d)). From the shape of the dislocation segments, we can see that the dislocation line in the vicinity of two interstitial jogs moves slower than those around vacancy jogs. FIG02(c) and FIG02(d) also suggest that the directions of interstitial clusters and vacancy tubes are determined by the nonconservative and conservative motions of jogs.

The motion of a large jog with a height of $15r_0$ (FIG03(a)) has also been investigated. Within the first $10t_0$, the dislocation segments as well as the jog pairs relax on the (001) plane, and disintegrate into small jogs (FIG03(b)). This decomposition is more obvious for large jogs than for small jogs (see FIG02(b) and FIG03(b)). It is also found in FIG03(b) that the dislocation segments around the negative z-axis decompose into small jogs more prominently than those around the positive z-axis. Under the external shear strain rate $\dot{\varepsilon}_{yz}$, similar to the above analysis, the nonconservative motion of the jogs occurs, producing a vacancy tube lying on a different $(1\bar{1}1)$ slip plane. Both FIG02 and FIG03 suggest that large jogs along the $\pm[\bar{1}10]$ directions on the (001) plane are not stable, decomposing into small ones. As indicated by the experiments of

Sriram *et al.* [1], cross-slip or double cross-slip is the major source of pinning points. Our simulations suggest a new mechanism responsible for creating jogs. In fact, the simulated configuration of the jogged screw dislocation line shown in FIG03(b) is very similar to the experimentally observed one (FIG02(b) in [1]). Based on the elasticity theory of dislocations [10], the dislocation elastic energies E_{el} satisfy E_{el}(screw)<E_{el}(mixed)<E_{el}(edge). Thus the jogs (edge dislocations) are not stable. They are first transformed into mixed ones (see FIG03(b)) and then are decomposed into small screw and edge segments. The edge segments will be the candidates for the pinning points.

At t=38t_0, we see the formation of a dipole around the small newly generated jog J_S with the jog height $2r_0$ (FIG03(c)). Due to the strong interaction between the segments L_{II} and L_{IV}, they can not pass by each other, indicating the shear strain $\varepsilon_{yz} = 3.49 \times 10^{-2}$ at t=38t_0 is not high enough to move these two segments. It is interesting to note that the simulated configuration of the dislocation dipole around the small, newly created jog J_S is very similar to the

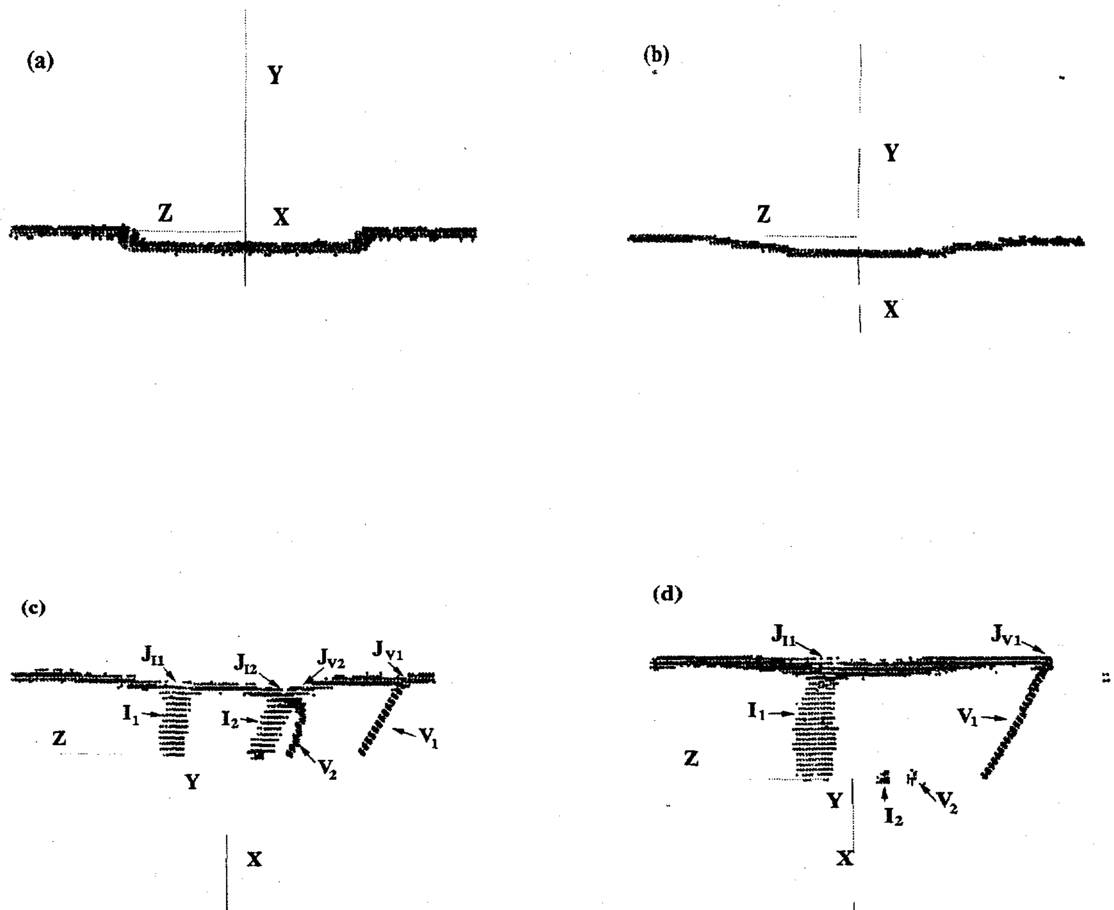

FIG02 (a) The initial configuration of a jogged screw dislocation with the height $4r_0$. (b) The decomposition configuration of the jogged screw dislocation at t=8t_0. (c) The jogged screw dislocation configuration at t=38t_0. The vacancy tube V_1 is aligned along the $[0\bar{1}\bar{1}]$ direction, and the interstitial cluster I_1 is approximately along the $[1\bar{1}\bar{2}]$ direction (negative x-axis). The interstitial cluster I_2 is approximately along the $[0\bar{1}\bar{1}]$ direction and the vacancy tube V_2 around the jog J_{V2} bends towards the interstitials cluster I_2. (d) At t=40t_0, the interstitial cluster I_2 and vacancy tube V_2 annihilate each other almost completely.

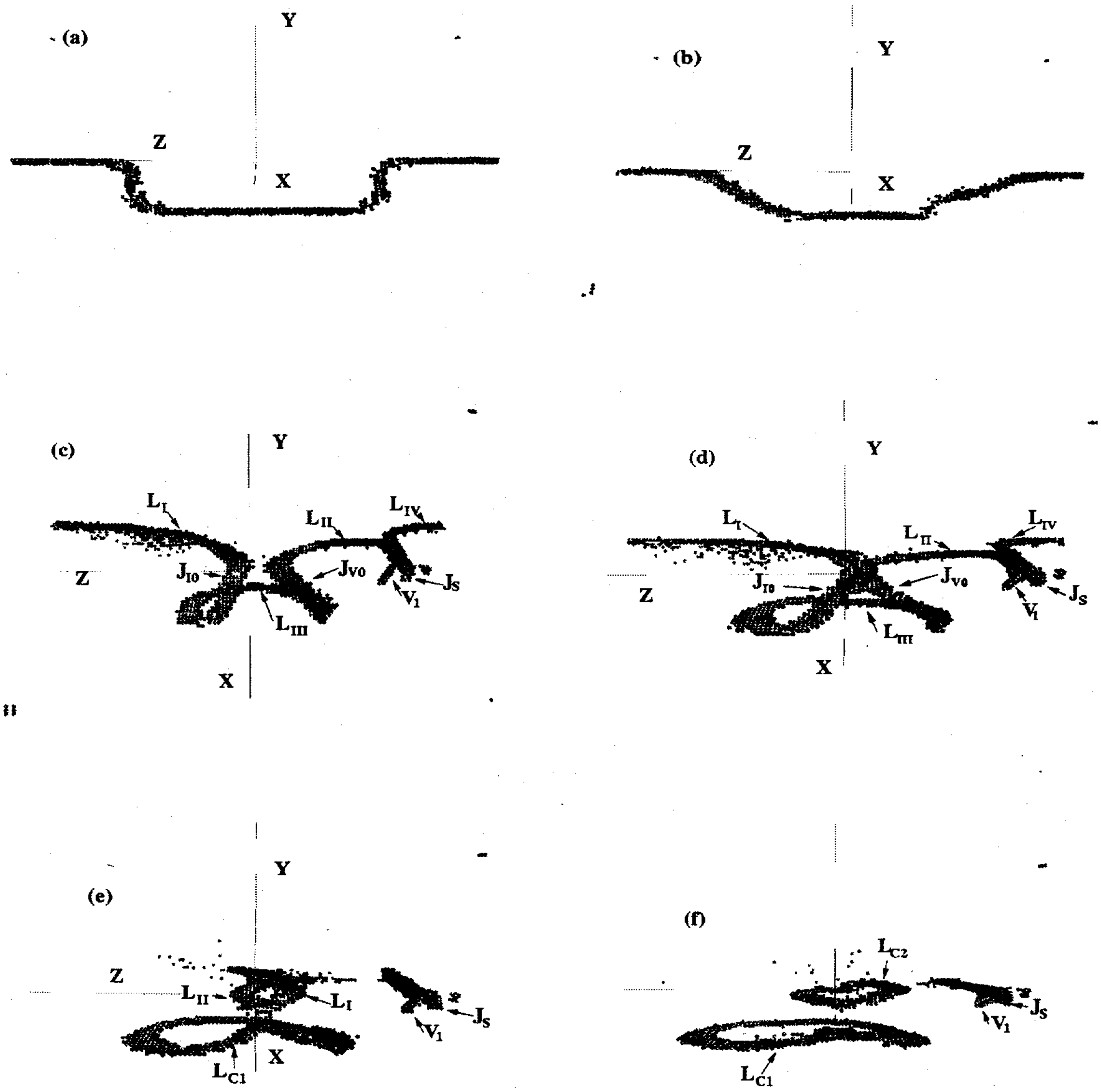

FIG03 (a) The initial configuration of a jogged screw dislocation with a height of $15r_0$. (b) The decomposed configuration of the jogged screw dislocation at $t=8t_0$. (c) At $t=38t_0$, the segments L_I, L_{II}, L_{III} and L_{IV} bow out on the $(1\bar{1}1)$ slip plane. A dipole has formed around the small, newly generated jog J_S. (d) At $t=40t_0$, the segments L_I and L_{II} glide on the $(1\bar{1}1)$ slip plane and almost contact each other. (e) At $t=46t_0$, the jogs J_{V0} and J_{I0} annihilate, and the segment L_{III} closes and creates a dislocation loop L_{C1} on the $(1\bar{1}1)$ slip plane. (f) At $t=50t_0$, the segments L_I and L_{II} pass each other and form a dislocation loop L_{C2} on the adjacent $(1\bar{1}1)$ slip planes. The rest of segments of L_I and L_{II} move out of the -yz free surface.

experimentally observed one shown in FIG09 in [1]. As shown in FIG03(c), the dislocation segments L_I, L_{II}, L_{III} and L_{IV} bow out significantly on different $(1\bar{1}1)$ slip planes. They exert additional forces on the original jogs J_{I0}, J_{V0} and on the newly generated smaller jog J_S. At $t=40t_0$, we see the segments L_I and L_{II} pass across each other on the adjacent $(1\bar{1}1)$ slip planes.

The dipole around the small, newly generated jog J_S, however, can not glide along the [110] direction. It can only grow along the $[1\bar{1}\bar{2}]$ direction on the $(1\bar{1}1)$ slip plane. At t=46t_0, the segment L_{II} detaches the dipole, gliding further along the [110] direction on the $(1\bar{1}1)$ slip plane (FIG03(d)). Moreover, the attractive interaction between jogs J_{V0} and J_{I0} have caused jogs J_{I0} and J_{V0} to move on the (001) plane conservatively along the ±[110] directions. Then these two jogs leave dislocation loop L_{C1} on the $(1\bar{1}1)$ slip plane (FIG03(e)). It is worth emphasizing the motion of the dislocation segments L_I and L_{II} shown in FIG03(c). These two segments bow out and glide towards each other on the primary $(1\bar{1}1)$ slip plane. At t=50t_0, these two segments form another dislocation loop L_{C2} on the $(1\bar{1}1)$ slip plane, above the dislocation loop L_{C1} (FIG03(f)). The rest of the segments of L_I and L_{II} move out of the *-yz* free surface. As shown in FIG03(f), the whole dislocation loop L_{C2} is not totally on the same $(1\bar{1}1)$ slip plane. The portion of the loop formed by the segment L_{II} is on the $(1\bar{1}1)$ plane while the rest of the loop formed by the segment L_I is on the adjacent $(1\bar{1}1)$ plane. The processes shown in FIG03 reveal a new atomic-level mechanism for a jogged dislocation to depin from a pair of jogs.

CONCLUSIONS

Based on our MD simulations, we obtain the following results on the jogged screw dislocations in γ-TiAl alloys. Jogs can be generated through the decomposition of large jogs into smaller jogs. Under the shear strain rate $\dot{\varepsilon}_{yz} = 5.4 \times 10^9 s^{-1}$, the critical height for a jog in the $[\bar{1}10]$ direction on the (001) plane to move nonconservatively is between $3r_0$ and $4r_0$. Interstitials and vacancies are created during the nonconservative motion of jogs. The dipole around a jog with a height $2r_0$ can exist stably. A jogged screw dislocation can depin from a pair of jogs by looping.

ACKNOWLEDGMENTS

We acknowledge using the framework of the SPaSM codes developed by P. S. Lomdahl, D. M. Beazley and other researchers. We acknowledge helpful discussions with Robb Thomson and are grateful to Brad Holian and Antonio Redondo for carefully reading the manuscript.

REFERENCES

[1] S. Sriram, D. M. Dimiduk, P. M. Hazzledine and V. K. Vasudevan, Phil. Mag. A **76**, p.553(1997).
[2] B. Viguer, K. J. Hemker, J. Bonneville, Phil.Mag.A **71**, p.1295(1995).
[3] N. Bird, G. Taylor and Y. Q. Sun, MRS proceedings, **364**, p.635(1995).
[4] M. Morris. Phil.Mag A **68**, p.237(1993).
[5] J. P. Hirth and J. Lothe, Theory of Dislocations, Second Edition, 1982.
[6] S. J. Zhou, D. L. Preston, P. S. Lomdahl and D. M. Beazley, Science, **279**, p.1525(1998).
[7] S. J. Zhou and D. L. Preston, Physica D (1999).
[8] D. Farkas, Modeling Simul. Mater. Sci. Eng., **2**, p.975(1994).
[9] M. Li and S. J. Zhou, to be published.
[10] D. Hull and D. J. Bacon, Introduction to Dislocations, 1986.